Characterisation and cytotoxicity studies of thiol-modified polystyrene microbeads doped with $[\{Mo_6X_8\}(NO_3)_6]^{2-}$ (X = Cl, Br, I)

Natalya A. Vorotnikova[a,b], Olga A. Efremova[c,d], Alphiya R. Tsygankova[a,e], Konstantin A. Brylev[a,e], Mariya V. Edeleva[b,f], Olga. G. Kurskaya[g], Andrew J. Sutherland[c*], Alexandr M. Shestopalov[g], Yuri V. Mironov[a,e] and Michael A. Shestopalov[a,b*]

[a]*Nikolaev Institute of Inorganic Chemistry SB RAS, 3 Acad. Lavrentiev Ave., 630090 Novosibirsk, Russian Federation. E-mail: shtopy@niic.nsc.ru; Fax: +7 (383) 330 94 89; Tel: +7 (383) 330 92 53*

[b]*Scientific Institute of Clinical and Experimental Lymphology, 2 Timakova Str., 630060 Novosibirsk, Russian Federation*

[c]*Chemical Engineering and Applied Chemistry, Aston University, Aston Triangle, Birmingham, B4 7ET, UK.*

[d]*Department of Chemistry, University of Hull, Cottingham Road, Hull, HU6 7RX, UK, E-mail: o.efremova@hull.ac.uk; Fax: +44 (0)148 246 6410; Tel: +44 (0)148 246 5417*

[e]*Novosibirsk State University, 2, Pirogova Str., 630090 Novosibirsk, Russian Federation*

[f]*Novosibirsk Institute of Organic Chemistry SB RAS, 9 Acad. Lavrentiev Ave, 630090 Novosibirsk, Russian Federation*

[g]*Research Institute of Experimental and Clinical Medicine, 2 Timakova Str., 630060 Novosibirsk, Russian Federation*

Keywords: molybdenum cluster complex, photoluminescence, polystyrene microbeads, cytotoxicity.

Abstract Halide octahedral molybdenum clusters $[\{Mo_6X_8\}L_6]^{n-}$ possess luminescent properties that are highly promising for biological applications. These properties are rather dependent on the nature of both the inner ligands X (*i.e.,* Cl, Br or I) and the apical organic or inorganic ligands L. Herein the luminescence properties and the toxicity of thiol-modified polystyrene micro-spheres (PS-SH) doped with $[\{Mo_6X_8\}(NO_3)_6]^{2-}$ (X = Cl, Br, I) were studied and evaluated using human epidermoid larynx carcinoma (Hep2) cell cultures. According to our data the photoluminescence quantum yield of $\{Mo_6I_8\}$@PS-SH is significantly higher (0.04) than that of $\{Mo_6Cl_8\}$@PS-SH (<0.005) and $\{Mo_6Br_8\}$@PS-SH (<0.005). Treatment of Hep2 cells with $\{Mo_6X_8\}$@PS-SH showed that all three types of doped microbeads had no significant effect on the viability and proliferation of the cells.

Introduction

Octahedral hexanuclear molybdenum cluster complexes of the general formula $[\{Mo_6X_8\}L_6]^{n-}$, where X (Cl, Br or I) are inner ligands within the cluster core $\{Mo_6X_8\}^{4+}$ and L are either organic or inorganic apical ligands, have been known for a more than half a century.[1, 2] However, the interest in these compounds was recently heightened due to the establishment of both the ability of these moieties to exhibit phosphorescence in the visible and near-infrared regions with high photoluminescence quantum yields (PLQYs)[3, 4] and their ability to generate singlet oxygen efficiently upon photoirradiation.[5] Such photophysical properties are essential assets for applications in bioimaging and photodynamic therapy. Despite the potential for utility in biomedical applications, the majority of known octahedral molybdenum cluster complexes are either insoluble in water or else are readily hydrolysed resulting in insoluble precipitates. Both

poor solubility and hydrolysis susceptibility hinder the biological applications of these metal clusters.

The most advantageous way to introduce biocompatibility to molybdenum metal cluster complexes is to support them within biocompatible, inert organic[3, 6, 7] or inorganic[8] matrices and render the resultant hybrid materials water miscible by modifying the matrix surfaces by attaching organic ligands having functional groups such as carboxyl, amino, amide, hydroxyl or epoxy.[9-12] Indeed, we recently showed that silica nanoparticles doped with molybdenum metal cluster complexes could enter the cells easily; they also showed high biocompatibility and low cellular toxicity in darkness.[13] However, upon photo-irradiation the cluster-containing nanoparticles demonstrated significant photo-induced cellular toxicity due to the generation of singlet oxygen (photo-dynamic cellular toxicity).

Additionally, we have also recently reported that thiol-functionalised polystyrene microbeads (PS-SH)[14] can be used as a polymeric ligand to bind molybdenum cluster complexes by replacement of labile ligands on the cluster complex cores.[6] Specifically $(Bu_4N)_2[\{Mo_6I_8\}(NO_3)_6]$ was incubated with PS-SH microbeads generating chemically stable and water dispersible material that emits in the red and near-infrared regions (*i.e.,* optical tissue window[15]) with a PLQY of about 0.04 and an emission lifetime up to several tens of microseconds. Importantly, the emission didn't show any quenching by either solvent or oxygen. Materials that combine such photoluminescence properties and dispersability in water have a high potential for bioimaging and biolabeling applications. However, for the materials to be used in such applications, it is crucial for them to be non-cytotoxic. Accordingly, in the work presented herein we describe the study of the cytotoxicity of a series of materials $\{Mo_6X_8\}$@PS-SH prepared by doping of PS-SH with the corresponding cluster complexes $(Bu_4N)_2[\{Mo_6X_8\}(NO_3)_6]$ (X = Cl (**1**), Br (**2**) or I (**3**)). The luminescence properties of complexes **1** and **2** and corresponding materials $\{Mo_6Cl_8\}$@PS-SH and $\{Mo_6Br_8\}$@PS-SH were also determined and compared with those of **3** and $\{Mo_6I_8\}$@PS-SH that were reported earlier.[6]

Experimental

Materials and Methods

All reagents and solvents employed were commercially available and used as received without further purification except for styrene, which was washed with a 1M aqueous solution of NaOH and dried over magnesium sulfate prior to use in polymerisation reactions. Thiol-containing microbeads (PS-SH) with 1% of a thiol containing monomer were obtained *via* a protocol reported previously.[14] The cluster complexes **1**-**3** were synthesised according to earlier reported procedures.[6, 16]

FTIR were recorded on a Bruker Vertex 80 in the form of KBr pellets. X-Ray powder diffraction patterns were recorded on a Shimadzu XRD 7000S powder diffractometer using copper irradiation. The thermal properties were studied on a Thermo Microbalance TG 209 F1 Iris (NETZSCH) in the temperature range 25–800 °C with a temperature gradient of 10 °C/min in a He flow (30 mL/min). Optical diffuse reflectance spectra were measured at room temperature on a Shimadzu UV-Vis-NIR 3101 PC spectrophotometer equipped with an integrating sphere and reproduced in the form of Kubelka–Munk theory. Elemental analysis was performed with a EuroVector EA3000 Elemental Analyser. The surfaces of the microparticles were characterised by scanning electron microscopy (SEM) using a JEOL JSM-5700 CarryScope microscope and by transmission electron microscopy (TEM) using a Libra 120 (Zeiss) transmission electron microscope. Optical densities in the MTT assay were recorded on a Multiskan FC (Thermo

scientific, USA). For each sample the average particle size and the standard deviation was determined on the basis of a selection of 50 random particles in the SEM image.
The molybdenum content in each cluster-containing sample was determined using a high resolution spectrometer iCAP-6500 (Thermo Scientific) with a cyclone type spray chamber and "SeaSpray" nebulizer. The spectra were obtained by axial plasma viewing. The standard operating conditions of the ICP-AES system are listed below: power – 1150 W, injector inner diameter – 3 mm, carrier argon flow – 0.7 L/min, accessorial argon flow – 0.5 L/min, cooling argon flow – 12 L/min, number of parallel measurements – 3, integration time – 5 s. The standard deviations were calculated on the basis of three parallel analyses with different amount of the samples. Deionised water with a resistance of about 18 MΩ was used in the preparation of the solutions. All chemical reagents were of analytical grade.

The general technique for preparation of {Mo_6X_8}@PS-SH (X = Cl, Br or I)

The preparation of {Mo_6X_8}@PS-SH (X = Cl, Br) was conducted using methodology described earlier for {Mo_6I_8}@PS-SH.[6] Specifically, cluster complex **1**, **2** or **3** (20 mg) was dissolved in CH_2Cl_2 (2 mL) and the resultant solution added to 2 mL of a CH_2Cl_2 suspension of thiol-modified polystyrene microbeads (100 mg/mL). The resultant mixture was sonicated for 5 minutes and then shaken at room temperature for 24 h. Centrifugation (RCF ~ 7000 g) was used to remove non-immobilised cluster complex from the suspension. The separated solid pellet was then resuspended in DMF (5 mL) using ultrasonication for 10 minutes, sedimented by centrifugation (10 min, 7000 g) and the supernatant was removed by decantation. This washing procedure was repeated four times with DMF and twice more with ethanol. To obtain a suspension of the microbeads in water the solid was washed with a 1% aqueous solution of PVP (M_n = 58000 g·mol^{-1}, 1% w/w, 3 mL). Then the solid was washed twice with water (5 mL) and, finally, suspended in water (2 mL). To determine the final concentration of the microbeads in water, a 1 mL aliquot of the suspension was dried to a constant mass at 100 °C.

Analytical measurements by the inductively coupled plasma atomic emission spectroscopy (ICP-AES)

The samples for ICP-AES were decomposed at 450 °C in accordance with the TG curves (Fig. 1). A sample (10-20 mg) and ~150 mg KOH (Reachim Ltd) were placed in a carbon glass crucible and heated up to 450 °C with the following the program: heated to 150 °C for 2 hours and maintained at this temperature for a further 2 hours then heated to 300 °C for 2 hours and maintained at this temperature for 2 hours, finally the temperature was raised to 450 °C for 2 hours and then maintained at this final temperature for 5 hours. After cooling, the sample was dissolved in water and transferred into a volumetric flask (V = 25 mL). Before the ICP-AES analysis was performed, all samples were diluted tenfold. To account for the matrix effect the reference solution was prepared in a similar manner to the investigated samples.

Luminescence measurements

To measure the emission properties of **1**, **2** and {Mo_6X_8}@PS-SH (X = Cl or Br) powders, the samples were placed between two non-fluorescent glass plates. The measurements were carried out at 298 K. The samples were excited by 355-nm laser pulses (6 ns duration, LOTIS TII, LS-2137/3). The corrected emission spectra were recorded on a red-light-sensitive multichannel photodetector (Hamamatsu Photonics, PMA-11). The emission decay was analysed by a streakscope system (Hamamatsu Photonics, C4334 and C5094). The emission quantum yields were determined by an Absolute Photo-Luminescence Quantum Yield Measurement System

(Hamamatsu Photonics, C9920-03), which comprised of an excitation Xenon light source (the excitation wavelength was 400 nm), an integrating sphere and a red-sensitive multichannel photodetector (Hamamatsu Photonics, PMA-12).

Cell culture

Human epidermoid larynx carcinoma (Hep2) were purchased from the State Research Centre of Virology and Biotechnology VECTOR, and cultured in EMEM supplemented with 10% fetal bovine serum, under a humidified atmosphere (5% CO_2 plus 95% air) at 37 °C.

MTT (3-[4,5-dimethylthiazol-2-yl]-2,5-diphenyltetrazolium bromide) colorimetric assays for cell proliferation

Cell culture was seeded on a 96-well plate with a concentration of $7 \cdot 10^3$ cells per well and incubated at 37 °C and 5% CO_2 for 24 hours. The media was then replaced with fresh media and cultured for 48 h with suspensions of $\{Mo_6X_8\}$@PS-SH (X= Cl, Br or I) or neat PS-SH microbeads with concentrations ranging from 0.006 to 3.25 mg/mL. The negative control was prepared identically but without any polymeric materials. 10 µL of the MTT solution (5 mg/mL) and 90 µL of media were added to each well, and the plates were incubated for 4 h. Thereafter the culture media were removed, the formazan formed was dissolved in 150 µL of dimethyl sulfoxide, vortexed, and formazan concentration was determined spectrophotometrically at 620 nm. The results are presented as the ratio of the optical density of the sample to the control. The experiment was repeated three times on separate days.

Results and discussion

Polystyrene microbeads doped with metal cluster complexes were obtained by the immobilisation of $(Bu_4N)_2[\{Mo_6Cl_8\}(NO_3)_6]$ **(1)** and $(Bu_4N)[\{Mo_6Br_8\}(NO_3)_6]$ **(2)** into thiol-containing polystyrene micro-spheres (PS-SH) in methylene chloride using methodology described previously for $\{Mo_6I_8\}$@PS-SH.[6] Specifically, the neat PS-SH micro-spheres swell readily in the methylene chloride, which allows ingress and subsequent interaction of the metal cluster complexes with the polymer matrix comprising the micro-spheres. The metal clusters react readily with the thiol groups of the PS-SH matrix resulting in the substitution of the labile nitrato ligands of the molybdenum cluster complexes by the thiol groups of the polymer matrix (Scheme 1). This leads to the irreversible binding of the metal clusters.

Evidence for molybdenum cluster complex incorporation into the PS-SH micro-spheres was assessed by UV/Vis diffuse reflectance spectroscopy. Here spectra of $\{Mo_6Cl_8\}$@PS-SH and $\{Mo_6Br_8\}$@PS-SH showed an enhanced optical absorption in comparison with pure PS-SH beads confirming the presence of molybdenum cluster complexes in the particles (Fig. 2). This is in agreement with the yellow colour of the samples. Elemental analysis of the materials $\{Mo_6X_8\}$@PS-SH (X = Cl, Br) did not show any detectable levels of nitrogen. Similarly, FTIR spectroscopy did not reveal any bands arising from NO_3^- ligand vibrations (Fig. 3). Altogether, these findings confirm the doping of PS-SH beads by the molybdenum metal cluster complexes **1** or **2** *via* the substitution of all of the nitrato ligands by the thiol-groups present within the beads.

In a more quantitative study, the content of molybdenum in $\{Mo_6X_8\}$@PS-SH (X = Cl, Br) was determined by ICP-AES. Since PS-SH is not soluble in water, inorganic acids, and mixtures thereof under ambient conditions, the pre-sintering of the material with alkali (KOH) was used to prepare samples for ICP-AES measurements. The accuracy of the chosen technique was verified by the "added-found" method. It was observed that the molybdenum content in the neat PS-SH is

less than that in pure potassium hydroxide (blank test). The experiment also showed that the "found" concentration coincided with the "added" concentration within the 95% confidence interval (Table 1). Thus, it can be concluded that the procedure of the sample preparation is suitable for determination of molybdenum in the $\{Mo_6X_8\}$@PS-SH (X = Cl, Br) samples, as it does not introduce the systematic errors in the analytical results.

ICP-AES analysis was carried out using the method of standard additions. This method of calibration eliminates the matrix effect, since the level and type of background signal in both the test sample and the reference sample are identical. This technique of sample pre-treatment was used to analyse the neat PS-SH and $\{Mo_6X_8\}$@PS-SH (X = Cl, Br). Mo content in the samples was found to be 0.31 ± 0.01% wt. for $\{Mo_6Cl_8\}$@PS-SH and 0.29 ± 0.003% wt. for $\{Mo_6Br_8\}$@PS-SH, which corresponds to the approximate ratio of $\{Mo_6X_8\}$ to thiol groups as 1:18 and 1:19, respectively.

SEM revealed that doping of the PS-SH microspheres with cluster units $\{Mo_6X_8\}$ (X = Cl or Br) did not cause any changes in size: the average diameters of the particles were 0.85±0.04 μm for $\{Mo_6Cl_8\}$@PS-SH sample, 0.88±0.05 μm for $\{Mo_6Br_8\}$@PS-SH sample and 0.86±0.06 μm for neat PS-SH. SEM images also did not show any changes in the morphology of the particles (Fig. 4). Namely, the surface of the particles remained smooth and the shape of the particles remained circular; no crystalline or other impurities was observed in the sample mats. In addition, XRPD confirmed that both $\{Mo_6Cl_8\}$@PS-SH and $\{Mo_6Br_8\}$@PS-SH materials have the same textural properties as neat PS-SH and that they are free from any crystalline impurities (Fig. 5). Confocal luminescence imaging (Fig. 6) showed clearly that the emission of molybdenum cluster complexes was indeed localised within the microspheres.

The detailed study of luminescence properties of cluster doped PS-SH was carried out on the dried powdered samples. The emission spectra of the $\{Mo_6X_8\}$@PS-SH (X = Cl, Br, I) materials are shown in Fig. 7, while the emission maximum wavelengths (λ_{em}), lifetimes (τ_{em}), and quantum yields (Φ_{em}) are summarised in Table 2. According to our data both **1** and **2** exhibit very weak luminescence in comparison with compound **3**. Φ_{em} values of materials $\{Mo_6Cl_8\}$@PS-SH and $\{Mo_6Br_8\}$@PS-SH are also significantly lower than that of $\{Mo_6I_8\}$@PS-SH. The emission maxima for $\{Mo_6X_8\}$@PS-SH are shifted about 20 nm for X = Cl and 55 nm for X = Br to the red region and 11 nm for X = I to the blue in relation to that of the corresponding cluster complexes **1**-**3**. These λ_{em} shifts along with irregular changes in emission lifetimes values and corresponding amplitudes and significant decrease of Φ_{em} for $\{Mo_6I_8\}$@PS-SH in comparison with **3** (see Table 2) are an additional indication of the change of apical ligand environment associated with the substitution of nitrato ligands by either thiol (–SH) or thiolate ($–S^-$) groups.

The organic compound 2,3-diphenyl-*para*-dioxene is well-established as a singlet oxygen trap (see Scheme 2), since the formation of ethylene glycol dibenzoate is easily discerned by means of ^{1}H NMR spectrometry.[17, 18] In our previous research, we assessed the photosensitising ability of the initial cluster compounds **1**-**3** using this molecular trap. It was shown that the relative efficiency of singlet oxygen generation increase in the order form **1** to **2** to **3**.[13] The similar experiment performed on the cluster doped polystyrene microbeads $\{Mo_6Cl_8\}$@PS-SH, $\{Mo_6Br_8\}$@PS-SH or $\{Mo_6I_8\}$@PS-SH in this work did not indicate any singlet oxygen generation by the particles. Moreover, photophysical parameters of solid sample of $\{Mo_6I_8\}$@PS-SH coincide with those of the water dispersion.[6] In combination these observations confirm that the PS-SH polymer matrix confers a strong shielding effect on the entrapped metal clusters against oxygen.

It is well established that polystyrene microspheres are highly biologically inert and are good materials for certain *in vitro* biological applications such as biolabeling and cellular delivery.[19]

However, we wished to establish that polystyrene microbeads doped with molybdenum cluster complexes had similarly low cytotoxicity values to values obtained from just undoped PS-SH micro-spheres. Accordingly cytotoxicity of both doped and undoped polystyrene micro-spheres was assessed by conducting a standard colorimetric cytotoxicity assay using 3-(4,5-dimethylthiazolyl-2)-2,5-diphenyltetrazolium bromide (MTT). In this MTT assay metabolically active cells reduce yellow tetrazolium MTT agent by the action of dehydrogenase enzymes producing purple formazan. The formazan is then dissolved and quantified by spectrophotometric means.[20]

Hep2 cells were incubated with differing concentrations (0.006 to 3.25 mg/mL) of $\{Mo_6X_8\}$@PS-SH (X = Cl, Br, I) or undoped PS-SH microspheres. The percentage of metabolically active cells post micro-sphere treatment was determined against the negative control (*i.e.,* the number of metabolically active cells in the non-treated samples). Our results show that neither PS-SH nor $\{Mo_6X_8\}$@PS-SH in concentrations up to ~0.20 mg/mL do not influence cell viability (Fig. 8), *i.e.*, the viability of the cells remain close to 100%. A subsequent increase of the polystyrene microbeads concentration up to 3.25 mg/mL resulted in a slight reduction (down to 80%) in the percentage of metabolically active cells. Due to the exceptionally low toxicity of our materials, the IC_{50} dose was not established. This study shows that there is no significant toxicity effect associated with the presence of any of our molybdenum cluster complexes in the polystyrene beads. This in turn means either or both: the metal cluster doesn't leach from the microbeads in physiological conditions and the low toxicity of the metal cluster complexes at the given concentrations.

In conclusion, we have shown that photoluminescent polystyrene beads doped with molybdenum cluster complexes, especially $\{Mo_6I_8\}$@PS-SH, are potentially excellent candidates for bio-imaging and bio-labeling applications. These materials show low toxicity in a broad range of concentrations and the incorporated cluster complexes emit in the optical tissue window brightly enough to be detected by many of the modern analytical tools. Going forward, future research should focus on further improving the photoluminescence quantum yields of the doped materials, for example by developing polymer matrices that bear other types of donor groups to bind metal clusters. It will also be interesting to evaluate loading the cluster complex doped polystyrene beads with biologically relevant cargos, *e.g.*, functionally active proteins, to facilitate cellular delivery of these entities, *i.e.*, beadfection.[19, 21, 22]

Acknowledgements

This work was supported by the Russian Science Foundation (Grant No. 14-14-00192). A.J. Sutherland is grateful to the Royal Society (Grant no. IE140281). O.A. Efremova is grateful to FP7 Marie Curie Inter-European Fellowship (Grant no. 327440). Also K.A. Brylev thanks the Japan Society for the Promotion of Science (JSPS) for a Post Doctoral Fellowship for Foreign Researchers and Prof. N. Kitamura (Hokkaido University) for the opportunity to study the luminescence properties.

References

[1] J.C. Sheldon, *Nature*, **1959**; 184, 1210.
[2] J.C. Sheldon, *J. Chem. Soc.*, **1962**, 410.
[3] K. Kirakci, P. Kubat, M. Dusek, K. Fejfarova, V. Sicha, J. Mosinger, K. Lang, *Eur. J. Inorg. Chem.*, **2012**, 3107.
[4] M.N. Sokolov, M.A. Mihailov, E.V. Peresypkina, K.A. Brylev, N. Kitamura, V.P. Fedin, *Dalton Trans.*, **2011**; 40, 6375.
[5] K. Kirakci, P. Kubat, J. Langmaier, T. Polivka, M. Fuciman, K. Fejfarova, K. Lang, *Dalton Trans.*, **2013**; 42, 7224.
[6] O.A. Efremova, M.A. Shestopalov, N.A. Chirtsova, A.I. Smolentsev, Y.V. Mironov, N. Kitamura, K.A. Brylev, A.J. Sutherland, *Dalton Trans.*, **2014**; 43, 6021.
[7] F. Grasset, F. Dorson, S. Cordier, Y. Molard, C. Perrin, A.M. Marie, T. Sasaki, H. Haneda, Y. Bando, M. Mortier, *Adv. Mater.*, **2008**; 20, 143.
[8] T. Aubert, F. Cabello-Hurtado, M.A. Esnault, C. Neaime, D. Lebret-Chauvel, S. Jeanne, P. Pellen, C. Roiland, L. Le Polles, N. Saito, K. Kimoto, H. Haneda, N. Ohashi, F. Grasset, S. Cordier, *J. Phys. Chem. C*, **2013**; 117, 20154.
[9] Q. Zhang, R.F. Huang, L.H. Guo, *Chin. Sci. Bull.*, **2009**; 54, 2620.
[10] Y.W. Zhang, M.K. Tiwari, M. Jeya, J.K. Lee, *Appl. Microbiol. Biotechnol.*, **2011**; 90, 499.
[11] H.S. Jung, D.S. Moon, J.K. Lee, *J. Nanomater.*, **2012**, Article ID 593471.
[12] E. Niemelä, D. Desai, Y. Nkizinkiko, J.E. Eriksson, J.M. Rosenholm, *Eur. J. Pharm. Biopharm.*, **2015**; 96, 11.
[13] Y. A. Vorotnikov, A. O. Solovieva, K. E. Trifonova, O. A. Efremova, N. A. Vorotnikova, K. A. Brylev, A. A. Krasilnikova, M. V. Edeleva, A. R. Tsygankova, A. I. Smolentsev, E. V. Vorontsova, P. A. Avrorov, L. V. Shestopalova, N. Kitamura, A. F. Poveshchenko, Y. V. Mironov, M.A. Shestopalov, unpublished work
[14] J.M. Behrendt, M. Afzaal, L.M. Alexander, M. Bradley, A.V. Hine, D. Nagel, P. O'Brien, K. Presland, A.J. Sutherland, *J. Mater. Chem.*, **2009**; 19, 215.
[15] R. Weissleder, *Nat. Biotechnol.*, **2001**; 19, 316.
[16] P. Braack, M.K. Simsek, W. Preetz, *Z. Anorg. Allg. Chem.*, **1998**; 624, 375.
[17] L. Gao, M.A. Peya, T.G. Gray, *Chem. Mater.*, **2010**; 22, 6240.
[18] M.A. Shestopalov, K.E. Zubareva, O.P. Khripko, Y.I. Khripko, A.O. Solovieva, N.V. Kuratieva, Y.V. Mironov, N. Kitamura, V.E. Fedorov, K.A. Brylev, *Inorg. Chem.*, **2014**; 53, 9006.
[19] J.M. Behrendt, D. Nagel, E. Chundoo, L.M. Alexander, D. Dupin, A.V. Hine, M. Bradley, A.J. Sutherland, *Plos One*, **2013**; 8.
[20] MTT Cell Prolifiration Assay (ATCC No. 30-1010K), American Type Culture Collection.
[21] L.M. Alexander, S. Pernagallo, A. Livigni, R.M. Sanchez-Martin, J.M. Brickman, M. Bradley, *Mol. Biosyst.*, **2010**; 6, 399.
[22] D. Nagel, J.M. Behrendt, G.F. Chimonides, E.E. Torr, A. Devitt, A.J. Sutherland, A.V. Hine, *Mol. Cell. Proteomics*, **2014**; 13, 1543.

Symbols and Abbreviations

PS-SH	Thiol-modified polystyrene micro-spheres
Hep2	Human epidermoid larynx carcinoma cell culture
PLQY	Photoluminescence quantum yield
FTIR	Fourier transform infrared spectroscopy
XRPD	X-ray powder diffraction
SEM	Scanning electron microscopy
TEM	Transmission electron microscopy
ICP-AES	Inductively coupled plasma atomic emission spectroscopy
RCF	Relative centrifugal force
DMF	*N*,*N*-Dimethylformamide
PVP	Poly(*N*-vinyl pyrrolidone)
EMEM	Eagle's minimum essential medium
MTT	(3-[4,5-Dimethylthiazol-2-yl]-2,5-diphenyltetrazolium bromide)

Table 1. ICP-AES data showing the "added-found" data for the content of molybdenum in $\{Mo_6X_8\}$@PS-SH

Sample neat PS-SH, mg	KOH, mg	Added Mo, μg	Found Mo, μg
20.5	18.1	30	33.0
20.6	417.9	30	39.9
20.3	440.4	0	4.2
20.2	418.7	0	3.4

Table 2. Spectroscopic and photophysical parameters of powdered samples **1-3** and $\{Mo_6X_8\}$@PS-SH. The excitation wavelength was 400 nm.

Sample	λ_{em} [nm]	τ_{em} [μs] (amplitude)	Φ_{em}
1	~ 765	τ_1 = 17 (0.14) τ_2 = 9.3 (0.02) τ_3 = 1.9 (0.84)	< 0.005
2	~ 785	τ_1 = 19 (0.25) τ_2 = 11 (0.20) τ_3 = 0.9 (0.55)	< 0.01
3[6]	~ 666	τ_1 = 96 (0.71) τ_2 = 26 (0.29)	26
$\{Mo_6Cl_8\}$@PS-SH	~ 745	τ_1 = 34.4 (0.07) τ_2 = 7.7 (0.16) τ_3 = 0.68 (0.77)	< 0.005
$\{Mo_6Br_8\}$@PS-SH	~ 730	τ_1 = 32.0 (0.14) τ_2 = 9.3 (0.32) τ_3 = 1.0 (0.54)	< 0.005
$\{Mo_6I_8\}$@PS-SH[6]	~ 677	τ_1 = 45 (0.15) τ_2 = 16 (0.4) τ_3 = 2.2 (0.45)	0.04

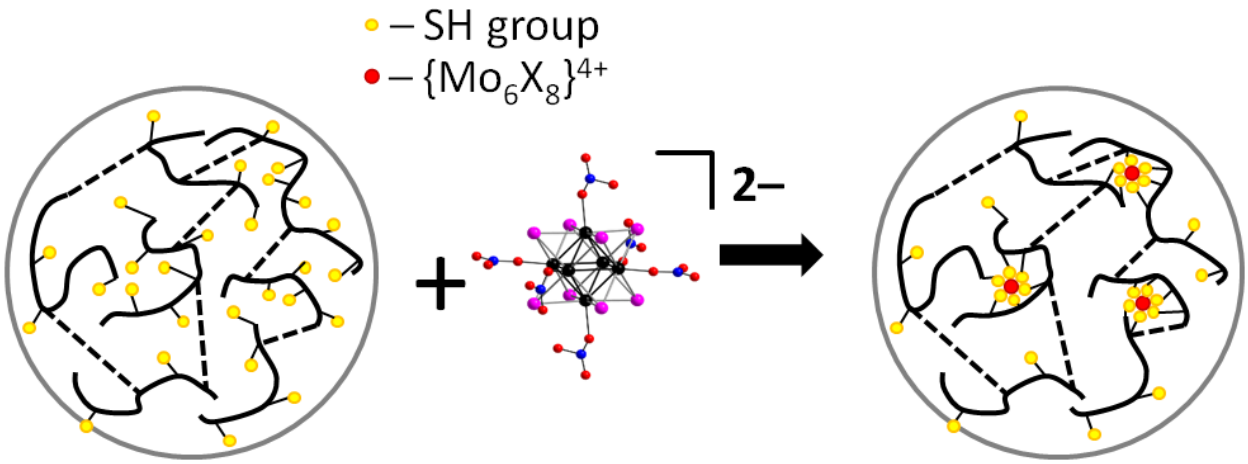

Scheme 1. Schematic representation showing the immobilization of $\{Mo_6X_8\}$-cluster units into PS-SH microbeads

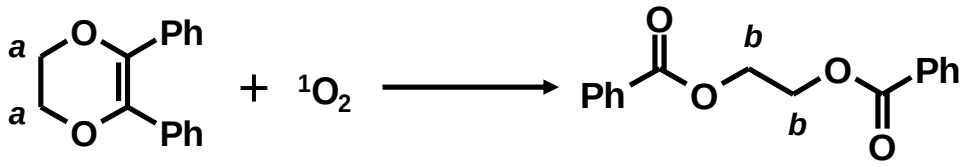

2,3-diphenyl-*para*-dioxene **ethylene glycol dibenzoate**

Scheme 2. Oxidation of 2,3-diphenyl-*para*-dioxene by $^1O_2$.

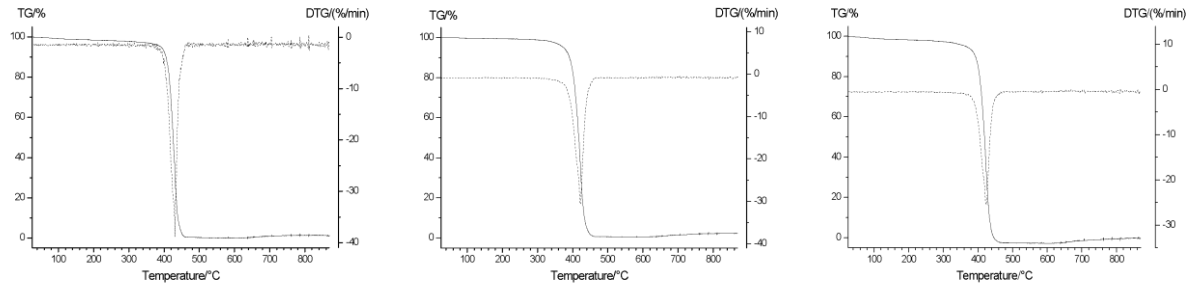

Figure 1. TG curves for {Mo_6Cl_8}@PS-SH (*left*), {Mo_6Br_8}@PS-SH (*middle*) and neat PS-SH (*right*)

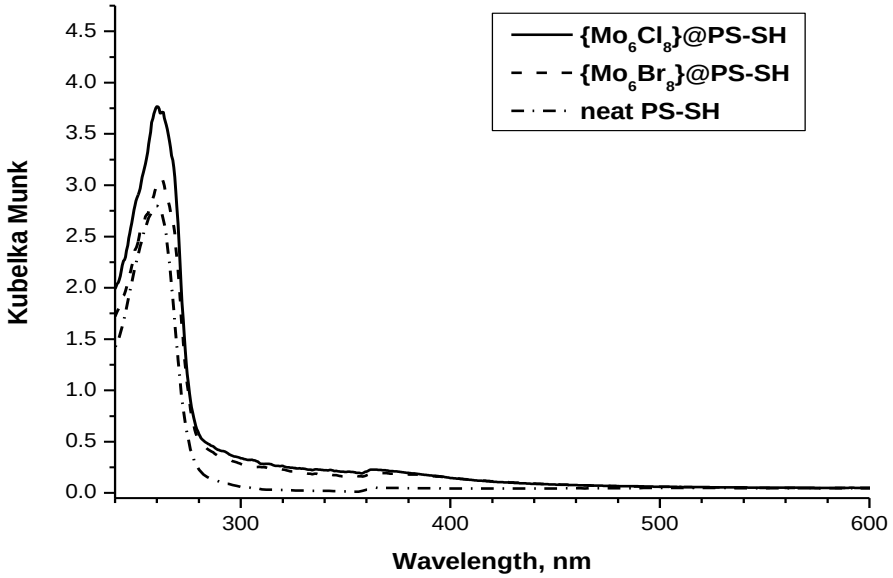

Figure 2. UV/Vis diffuse reflectance spectra of {Mo_6Cl_8}@PS-SH, {Mo_6Br_8}@PS-SH and neat PS-SH

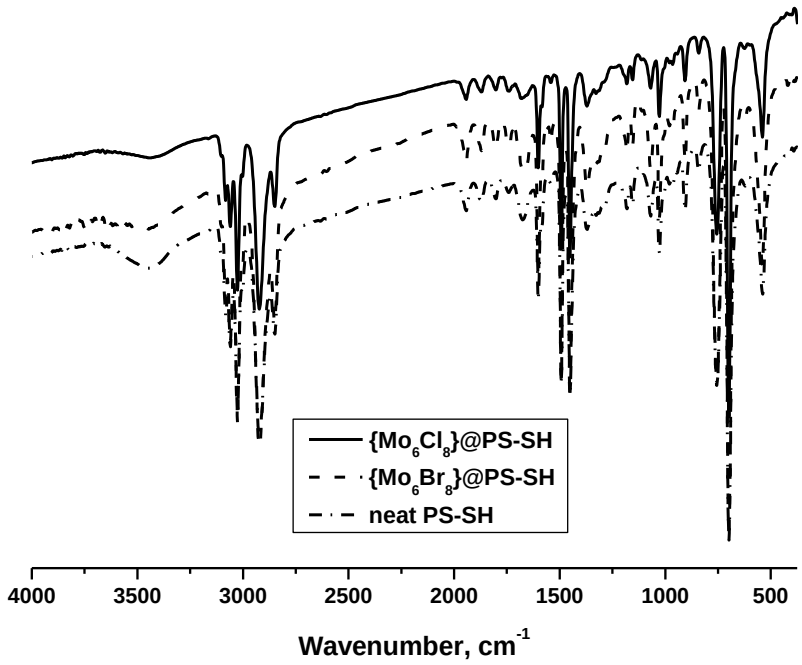

Figure 3. FTIR spectra of $\{Mo_6Cl_8\}$@PS-SH, $\{Mo_6Br_8\}$@PS-SH and neat PS-SH

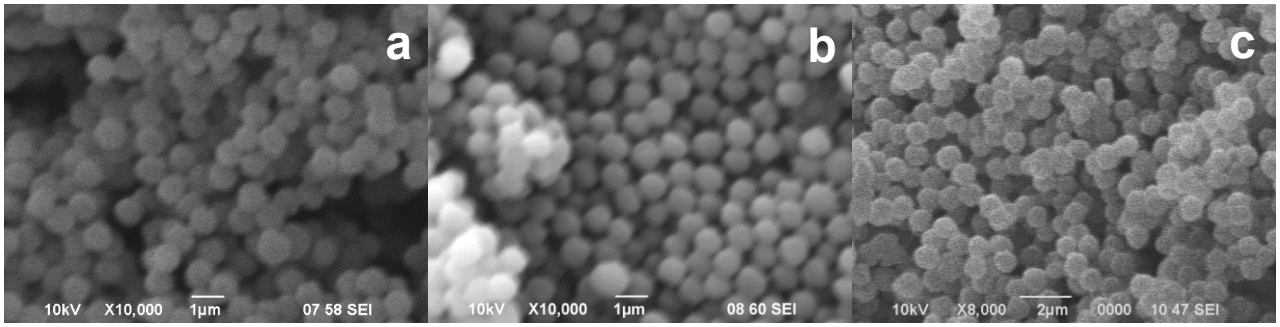

Figure 4. SEM image of $\{Mo_6Cl_8\}$@PS-SH (a), $\{Mo_6Br_8\}$@PS-SH (b) and neat PS-SH (c)

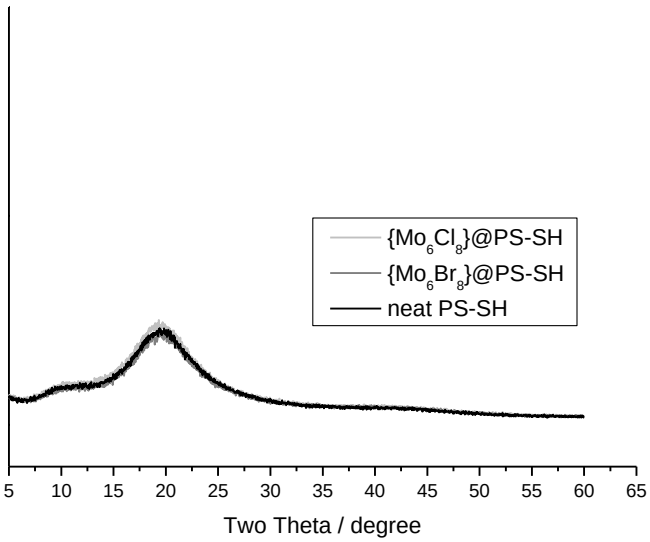

Figure 5. XRPD for $\{Mo_6Cl_8\}$@PS-SH, $\{Mo_6Br_8\}$@PS-SH and neat PS-SH

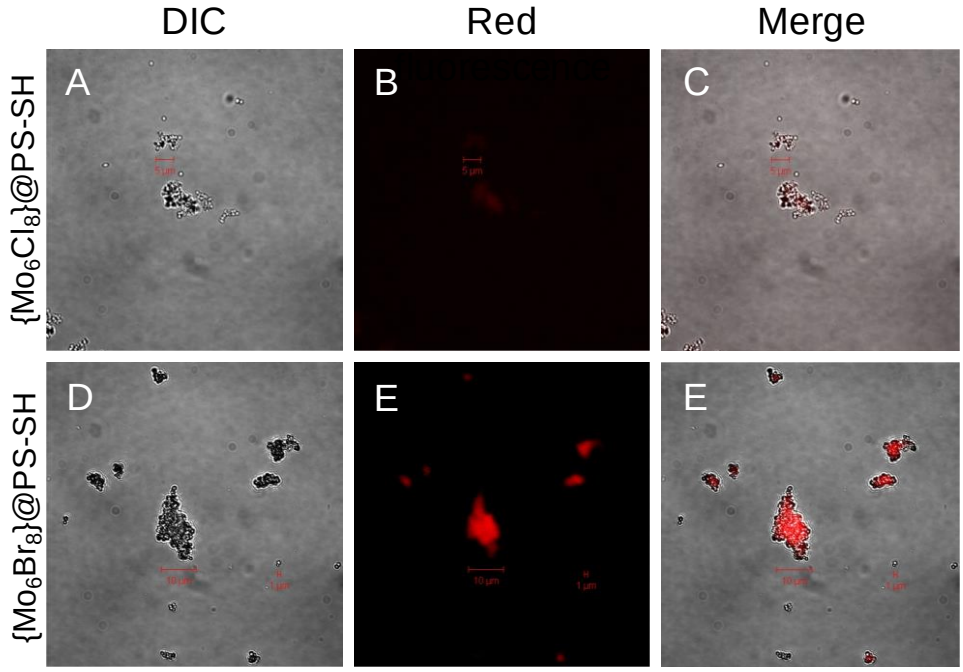

Figure 6. Confocal fluorescence microscopy imaging of $\{Mo_6Cl_8\}$@PS-SH and $\{Mo_6Br_8\}$@PS-SH materials showing: differential interference contrast (DIC) **(A, D)**, red fluorescence **(B, E)**, and merged images **(C, F)**. Red bars indicate 10 µm. Zoom x100

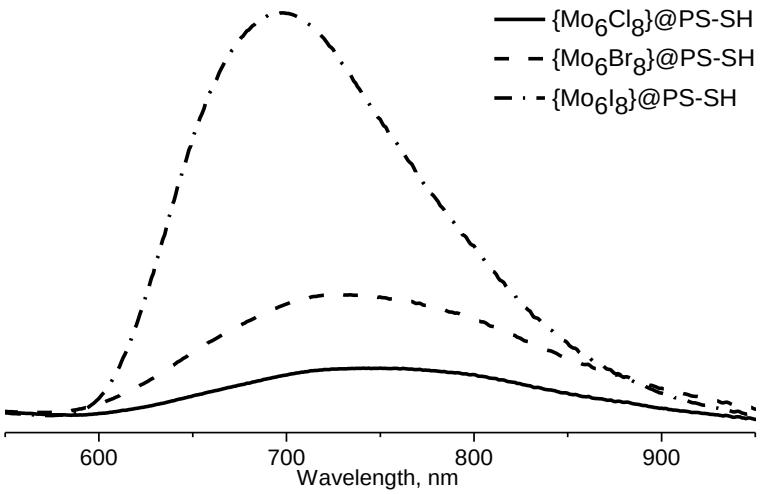

Figure 7. Photoemission spectra of powdered samples of $\{Mo_6X_8\}$@PS-SH (X = Cl, Br or I)

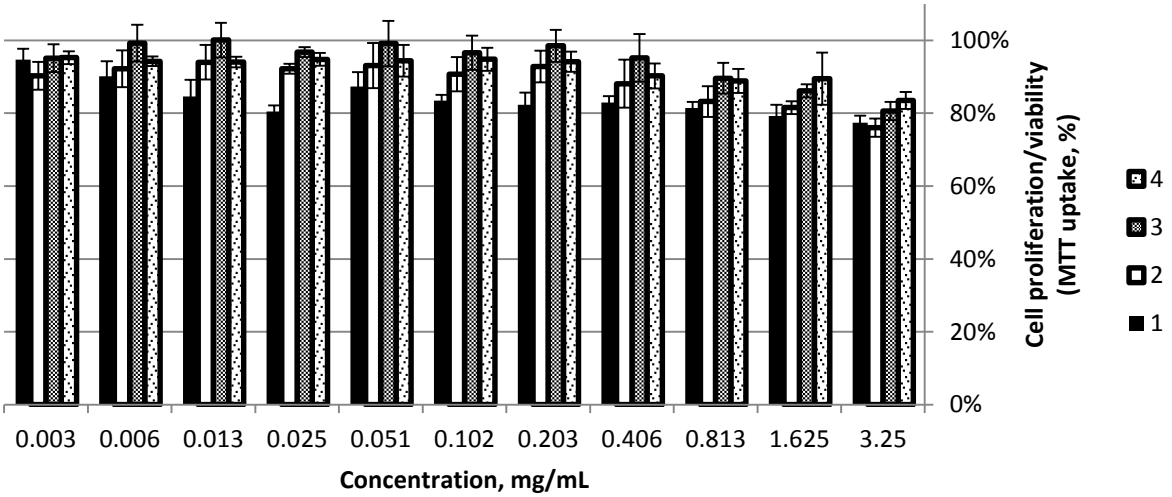

Figure 8. Influence of polymeric materials $\{Mo_6X_8\}$@PS-SH on Hep-2 cell proliferation: 1 – neat PS-SH, 2 – $\{Mo_6Cl_8\}$@PS-SH, 3 – $\{Mo_6Br_8\}$@PS-SH, 4 – $\{Mo_6I_8\}$@PS-SH